



Rigid body motions capturing by means of wearable inertial and magnetic MEMS sensors assembly: From the reconstitution of the posture toward the dead reckoning: an application in Bio-logging

Hassen Fourati, Nouredine Manamanni, Lissan Afilal, Yves Handrich

► To cite this version:

Hassen Fourati, Nouredine Manamanni, Lissan Afilal, Yves Handrich. Rigid body motions capturing by means of wearable inertial and magnetic MEMS sensors assembly: From the reconstitution of the posture toward the dead reckoning: an application in Bio-logging. MEMS: Fundamental Technology and Applications (Devices, Circuits, and Systems), CRC Press, pp.313-329, 2013, Devices, Circuits, and Systems (Book 15), 978-1466515819. hal-00909138

HAL Id: hal-00909138

<https://hal.science/hal-00909138>

Submitted on 9 Dec 2013

HAL is a multi-disciplinary open access archive for the deposit and dissemination of scientific research documents, whether they are published or not. The documents may come from teaching and research institutions in France or abroad, or from public or private research centers.

L'archive ouverte pluridisciplinaire **HAL**, est destinée au dépôt et à la diffusion de documents scientifiques de niveau recherche, publiés ou non, émanant des établissements d'enseignement et de recherche français ou étrangers, des laboratoires publics ou privés.

Rigid body motions capturing by means of wearable inertial and magnetic MEMS sensors assembly: from the reconstitution of the posture toward the dead reckoning: an application in Bio-logging

Hassen Fourati^a, Noureddine Manamanni^{b,*}, Lissan Afilal^b, Yves Handrich^c

^a *Grenoble Images Parole Signal Automatique (GIPSA-lab)*

*CNRS : UMR5216 – Université Joseph Fourier - Grenoble I – Université Pierre-Mendès-France
- Grenoble II – Université Stendhal - Grenoble III – Institut Polytechnique de Grenoble -
Grenoble Institute of Technology*

NeCS (INRIA Grenoble Rhône-Alpes / Gipsa-lab)

*CNRS : UMR5216 – INRIA – Gipsa-lab – Université Joseph Fourier - Grenoble I – Institut
National Polytechnique de Grenoble (INPG)*

^b *CReSTIC, URCA, EA 3804 – Université de Reims Champagne-Ardenne*

UFR SEN, Moulin de la Housse Bat 12, 51687 Reims Cedex 2 France

{name.surname}@univ-reims.fr (*Corresponding author)

^c *Institut Pluridisciplinaire Hubert CURIEN / Département Ecologie, Physiologie et Ethologie*

UMR 7178 CNRS – Université de Strasbourg

23 rue du læss – BP28 67037 Strasbourg cedex 2, France.

yves-jean-handrich@c-strasbourg.fr

1. INTRODUCTION

The rigid body attitude and orientation estimation problems are highly motivated from various applications. For example, in rehabilitation and biomedical engineering [1], the attitude is used in stroke rehabilitation exercises to record patient's movements in order to provide adequate feedback for the therapist. In human motion tracking and biomechanics [2], the attitude serves as a tool for physicians to perform long-term monitoring of the patients and to study human movements during everyday activities. Moreover, the attitude estimation is extensively used in tracking of handheld microsurgical instrument [3]. In aerial and marine vehicles [4], the attitude is used to achieve a stable controller.

Recently, the problem of attitude and orientation tracking has been treated in another scientific field: The Bio-logging. This latter stands in the intersection of animal behavior and bioengineering and aims at obtaining new information from the natural world and providing new insights into the hidden lives of animal's species [5], [6]. Bio-logging generally involves a free-ranging animal-attached electronic device (called also bio-logger) that records aspects of the animal's biology (behavior, movement, physiology) [7], [8] and its environment. Thirty years ago, several tagging technologies such as satellite tracking (the Argos system) [9] and Time-Depth-Recorders (TDRs) [10] have been used to provide a basic knowledge on the function of free-ranging organisms. The recent advances in electronic miniaturization, sensors and digital information processing allowed researchers studying animal's biology with a high level of detail and across the full range of ecological scales.

Many marine and terrestrial animals are studied during their daily activities. The posture and orientation tracking of these free-ranging animals represents one of the recent biology aspects studied in Bio-logging. Indeed, some scientific researches started to focus on this topic using low-cost sensors based on Micro Electro-Mechanical System (MEMS) technology as a 3-axis accelerometer and a 3-axis magnetometer. The obvious advantage of this new approach is the gain access to the third dimension space, which is the key to a good understanding of the diving strategies observed in these predators [11]. The main question to answer is how it is possible to extract the gravity components of the body animal [12-14]? This information is exploited after to deduce the corresponding posture (attitude) and consequently the Dynamic Body Acceleration. In this chapter, we propose the addition of 3-axis gyroscope measurements to the sensors already used (3-axis accelerometer and 3-axis magnetometer) in Bio-logging. The use of gyroscope with

accelerometer and magnetometer, mounted in triad configuration, in Bio-logging has never been done before in our knowledge. In our opinion, it can improve the estimation precision of the attitude especially during dynamic situation of the animal motion [4], [15], [16]. The main idea of the algorithm is to use a complementary filter coupled with a Levenberg Marquardt Algorithm (LMA) to process the measurements from a 3-axis gyroscope, a 3-axis magnetometer and a 3-axis accelerometer. The proposed approach combines a strap-down system, based on the time integral of the angular velocity, with the LMA that uses the Earth's magnetic field and the gravity vector to compensate the attitude predicted by the gyroscope. It is important to note that the resulting structure is complementary: high bandwidth rate gyro measurements are combined with low bandwidth vector observations (gravity and Earth's magnetic field) to provide an accurate attitude estimate. Thanks to the knowledge of the estimated attitude, it is now possible to reconstitute the Dynamic Body Acceleration of the animal in order to evaluate its daily diary [14] (sleeping, walking/flying, running, and hunting) and provide important insights into some of the stresses faced by free-ranging animals especially the king penguin and badger.

In the second part of the chapter, the problem of 3D position estimation in the case of pedestrian locomotion is addressed. The final goal would be to apply this work in Bio-logging to reconstruct the trajectory of animal. Previous works in this domain have focused only on marine animals using a 3-axis accelerometer and speed sensor to estimate the 3D position [14]. In this chapter, we are interested to the case of terrestrial animal. Based only on measurements provided by a 3-axis accelerometer, a 3-axis magnetometer and a 3-axis gyroscope (Inertial Measurement Unit, a position estimation approach is proposed. A dead reckoning approach is used where the Dynamic Body Acceleration is integrated to estimate at first the linear velocity and then the position. A complementary filter approach is used to estimate the body attitude that is necessary to reconstruct the Dynamic Body Acceleration. An experimental evaluation of the proposed approach is carried out in the case of human locomotion and where an Inertial Measurement Unit is attached to the foot of the subject.

This chapter is organized as follows: section 2 describes the problem statement and our motivations for motion estimation in the case of the attitude and position in Bio-logging. Section 3 details the attitude parameterization and the sensor measurement models used in this work. Section 4 details the structure of the proposed complementary filter for the attitude estimation. Section 5 is devoted to experimental results to illustrate the effectiveness of the proposed

algorithm. Section 6 introduces some concepts about 3D position estimation approach in the case of pedestrian locomotion with our first experimental results. Finally, section 7 summarizes the main conclusions of the chapter.

2. MOTIVATIONS AND PROBLEM FORMULATION

Recent technological advances have revolutionized the approach of the animals in their environment, and have enabled researchers in biology and eco-physiology to leave their laboratories to study these adaptations on the animal models living freely in their natural environment. Bio-logging has been introduced as the science that studies the behavior, physiology, ecology and environment properties of free-living animals (bioclimatic, global change, etc...) that are often beyond the border of our visibility or experience. Bio-logging has found its origin in the marine environment [10] and has diversified into the study of flying and terrestrial species. This scientific area refers often to the study of free-ranging animals in their natural environment through miniaturized electronic devices (called also bio-loggers [17]) usually attached to their bodies. These systems measure and record biological parameters or physico-chemical properties related to the individual and / or its environment using various types of sensors (luminosity, pressure, velocity, etc...). The loggers provide time tracking of physical and biological parameters over periods ranging from several hours to several months or sometimes a year and at sampling rates ranging from minutes to several times per second. The King penguin and badger are the major biological models studied in Strasbourg University thanks to the Bio-logging technology. Biologists are recently interested to reconstruct the motions of these animals (3D attitude and position) under several acceleration profiles, to be able to study their behaviour during long periods.

In this chapter, we are interested to:

- Firstly, propose a robust alternative approach to estimate the movement patterns (attitude or orientation) of rigid body, which represents the animal body, to be applied after in the case of penguin (see Fig. 1). To achieve this goal, we use a wearable inertial and magnetic MEMS sensors assembly based on a 3-axis accelerometer, a 3-axis magnetometer and a 3-axis gyroscope (Inertial Measurement Unit). Furthermore, the estimated attitude is used to calculate three components of Dynamic Body Acceleration (DBA) of the animal, which provides for biologists important information about the energy budgets of free-living animals.

- Secondly, we address the problem of 3D position estimation in the case of human pedestrian locomotion, based on attitude and DBA estimations. The goal is to obtain results that remain promising to reconstruct the animal position for an application in Bio-logging.

3. MATERIALS AND METHODS

3.1. RIGID BODY ATTITUDE AND COORDINATE SYSTEMS

A rigid body is considered as a solid formed from a finite set of material points with deformable volume [18]. Generally, the rigid body attitude represents the direction of its principal axes relative to a reference coordinate system and its dynamics expresses the change of object orientation. In the navigation field, the attitude estimation problem requires the transformation of measured and computed quantities between various frames. The rigid body attitude is based on measurements gained from sensors attached to this latter. Indeed, inertial sensors (accelerometer, gyroscope, etc...) are attached to the body-platform and provide inertial measurements expressed relative to the instrument axes. In most systems, the instrument axes are nominally aligned with the body-platform axes. Since the measurements are performed in the body frame, we describe in Fig. 2 the orientation of the body-fixed frame $B(X_B, Y_B, Z_B)$ with respect to the Earth-fixed frame $N(X_N, Y_N, Z_N)$, which is tangent to the Earth's surface (Local Tangent Plane, LTP). This local coordinate is particularly useful to express the attitude of a moving rigid body on the surface of the Earth [19]. The X_N -axis points true north. The Z_N -axis points towards the interior of the Earth, perpendicular to the reference ellipsoid. The Y_N -axis completes the right-handed coordinate system, pointing east (NED: North, East, Down).

3.2. MATHEMATICAL MODEL OF ATTITUDE REPRESENTATION

In this chapter, we use the quaternion algebra to describe the rigid body attitude. The unit quaternion, denoted by q , is expressed as:

$$q = q_0 + q_{vect} = q_0 1 + q_1 i + q_2 j + q_3 k \in H \quad (1)$$

where $q_{vect} = q_1 i + q_2 j + q_3 k$ represents the imaginary vector, q_0 is the scalar element and H can be written such as:

$$H = \left\{ q / q^T q = 1, q = \begin{bmatrix} q_0 & q_{vect}^T \end{bmatrix}^T, q_0 \in \mathbb{R}, q_{vect} = \begin{bmatrix} q_1 & q_2 & q_3 \end{bmatrix}^T \in \mathbb{R}^{3 \times 1} \right\} \quad (2)$$

The rotation matrix in term of quaternion can be written as:

$$M_N^B(q) = \begin{bmatrix} 2(q_0^2 + q_1^2) - 1 & 2(q_1q_2 + q_0q_3) & 2(q_1q_3 - q_0q_2) \\ 2(q_1q_2 - q_0q_3) & 2(q_0^2 + q_2^2) - 1 & 2(q_0q_1 + q_2q_3) \\ 2(q_0q_2 + q_1q_3) & 2(q_2q_3 - q_0q_1) & 2(q_0^2 + q_3^2) - 1 \end{bmatrix} \quad (3)$$

We invite the reader to refer to [20] for a more details about quaternion algebra.

3.3. 3-AXIS INERTIAL/MAGNETIC SENSORS PACKAGE MEASUREMENT MODELS

The sensors configuration consists of a 3-axis accelerometer, a 3-axis magnetometer and a 3-axis gyroscope containing MEMS technologies. A detailed study of these sensors is given in [21].

3.3.1. 3-axis accelerometer

An accelerometer measures the acceleration of the object that it supports. If three accelerometers are mounted in orthogonal triad in a rigid body, such that their sensitive axes coincide with the principal axes of inertia of the moving body. The output of a 3-axis accelerometer in the body-fixed frame (B) is given by the following measurement vector [22]:

$$f = M_N^B(q)(a - G) + \delta_f \quad (4)$$

where $G = [0 \ 0 \ g]^T$ and $a = [a_x \ a_y \ a_z]^T$ represent, respectively, the gravity vector and the Dynamic Body Acceleration (DBA) of the rigid body, given in the Earth-fixed frame (N).

$\delta_f \in \mathfrak{R}^3$ is a noise vector assumed to be independent, white and Gaussian. $M_N^B(q)$ is the rotation matrix defined in (3) and reflecting the transition between the frames (N) and (B).

3.3.2. 3-axis magnetometer

A magnetometer, sometimes called magnetic compass is a device for measuring the direction and intensity of a magnetic field and especially the Earth's magnetic field. The output of a 3-axis magnetometer in the body-fixed frame (B) is given by the following measurement vector [22]:

$$h = M_N^B(q)m + \delta_h \quad (5)$$

where m is the magnetic field expressed in the Earth-fixed frame (N) by:

$$m = [m_x \quad 0 \quad m_z]^T = [\|m\|\cos(I) \quad 0 \quad \|m\|\sin(I)]^T \quad (6)$$

δ_h is a white Gaussian noise and $M_N^B(q)$ is the rotation matrix expressed in (3). Currently, the parameters of the theoretical model of the geomagnetic field m closest to reality can be deduced from [23].

3.3.3. 3-axis gyroscope

A gyroscope is an inertial sensor that measures the angular velocity of reference attached to the sensor compared to an absolute reference frame along one or more axes [24]. The output of a 3-axis gyroscope in the body-fixed frame (B) is given by the measurement vector [22]:

$$\omega_G = \omega + b + \delta_G \quad (7)$$

where $\omega \in \mathfrak{R}^3$ is the real angular velocity, $b \in \mathfrak{R}^3$ is a slowly time varying function [21] called also bias and δ_G is a white Gaussian noise.

4. DESIGN APPROACH FOR ATTITUDE ESTIMATION: COMPLEMENTARY FILTER

In this chapter, the objective is to design an attitude estimation algorithm based on inertial and magnetic MEMS sensors. The application in mind is related to a free-ranging animal case in Bio-logging [25]. By considering the rigid body kinematic model, a complementary filter is proposed in order to take advantage from the good short-term precision given by rate gyros integration and the reliable long-term accuracy provided by accelerometer and magnetometer measurements.

This leads to better attitude estimates [4]. It is important to note that the resulting approach structure is complementary: high bandwidth rate gyro measurements are combined with low bandwidth vector observations to provide an accurate attitude estimate [26].

4.1. RIGID BODY KINEMATIC MOTION EQUATION

The rigid body motion can be described by the attitude kinematic differential equation [27], which represents the time rate of attitude variation, expressed in a quaternion term q , as a result of the rigid body angular rates measured by the gyroscope:

$$\dot{q} = \frac{1}{2} \begin{bmatrix} -q_{vect}^T \\ I_{3 \times 3} q_0 + [q_{vect}^\times] \end{bmatrix} \omega_G \quad (8)$$

where

- $q = [q_0 \quad q_{vect}^T]^T$ is the unit quaternion that denotes the mathematical representation of the rigid body attitude between two frames: body-fixed frame (B) and Earth-fixed frame (N).

Note that $q_{vect} = [q_1 \quad q_2 \quad q_3]^T$ represents the vector part of q . It is customary to use quaternions instead of Euler angles since they provide a global parameterization of the body orientation, and are well-suited for calculations and computer simulations.

- ω_G represents the angular velocity vector expressed in (B) and $I_{3 \times 3}$ is the identity matrix of dimension 3.
- $[q_{vect}^\times]$ represents the standard vector cross-product (the skew-symmetric matrix) which is defined such as:

$$[q_{vect}^\times] = \begin{bmatrix} q_1 \\ q_2 \\ q_3 \end{bmatrix}^\times = \begin{bmatrix} 0 & -q_3 & q_2 \\ q_3 & 0 & -q_1 \\ -q_2 & q_1 & 0 \end{bmatrix} \quad (9)$$

4.2. THE DESIGN STATE MODEL

Let us consider the following system model (S_1) composed of (8) with the output y that represents the linear measurement model. The output $y \in \mathfrak{R}^6$ of this system is built by stacking the accelerometer and magnetometer measurements.

$$(S_1): \begin{cases} \begin{bmatrix} \dot{q}_0 \\ \dot{q}_1 \\ \dot{q}_2 \\ \dot{q}_3 \end{bmatrix} = \frac{1}{2} \begin{bmatrix} -q_{vect}^T \\ I_{3 \times 3} q_0 + [q_{vect}^\times] \end{bmatrix} \omega_G = \frac{1}{2} \begin{bmatrix} -q_1 \omega_{Gx} - q_2 \omega_{Gy} - q_3 \omega_{Gz} \\ q_0 \omega_{Gx} - q_3 \omega_{Gy} + q_2 \omega_{Gz} \\ q_3 \omega_{Gx} + q_0 \omega_{Gy} - q_1 \omega_{Gz} \\ q_1 \omega_{Gy} - q_2 \omega_{Gx} + q_0 \omega_{Gz} \end{bmatrix} \\ y = [f_x \quad f_y \quad f_z \quad h_x \quad h_y \quad h_z]^T \end{cases} \quad (10)$$

By considering the rigid body kinematic equation and the linear measurement model y , the

proposed system (S_1) can take advantage from the good short term precision given by the rate gyros integration and the reliable long term accuracy provided by accelerometers and magnetometers measurements fusion [26], [28], which leads to improve the quaternion estimation.

4.3. ATTITUDE COMPLEMENTARY FILTER

The aim of this approach is to ensure a compromise between the accuracy provided by short-term integration of the gyroscope data and the long-term measurements precision obtained by the accelerometer and the magnetometer. To compensate for the drifts on the estimated quaternion that are observed during the integration of the differential equation (8), a correction term T is introduced in this equation based on a quaternion product \otimes . We propose the following complementary filter:

$$(F): \begin{bmatrix} \dot{\hat{q}}_0 \\ \dot{\hat{q}}_1 \\ \dot{\hat{q}}_2 \\ \dot{\hat{q}}_3 \end{bmatrix} = \frac{1}{2} \begin{bmatrix} -\hat{q}_1\omega_x - \hat{q}_2\omega_y - \hat{q}_3\omega_z \\ \hat{q}_0\omega_x - \hat{q}_3\omega_y + \hat{q}_2\omega_z \\ \hat{q}_3\omega_x + \hat{q}_0\omega_y - \hat{q}_1\omega_z \\ \hat{q}_1\omega_y - \hat{q}_2\omega_x + \hat{q}_0\omega_z \end{bmatrix} \otimes T \quad (11)$$

where $\hat{q} = [\hat{q}_0 \quad \hat{q}_1 \quad \hat{q}_2 \quad \hat{q}_3]^T \in \mathfrak{R}^4$ represents the estimated quaternion. The correction term T is calculated from a fusion approach of accelerometer and magnetometer data. The quaternion product introduced in (11) allows to merge the magnetic and inertial measurements.

Let us present the method for calculating the correction term T . We consider the modeling error $\delta(\hat{q}) = (y - \hat{y})$. The estimated output is given by \hat{y} :

$$\hat{y} = \begin{bmatrix} \hat{f}_x & \hat{f}_y & \hat{f}_z & \hat{h}_x & \hat{h}_y & \hat{h}_z \end{bmatrix}^T \quad (12)$$

Measurements of the estimated accelerations \hat{f}_x , \hat{f}_y and \hat{f}_z can be calculated by assuming that the Dynamic Body Acceleration a is low ($\|a\|_2 \ll \|G\|_2$) [29]. Thus we obtain:

$$\hat{f} = \begin{bmatrix} 0 & \hat{f}_x & \hat{f}_y & \hat{f}_z \end{bmatrix}^T = \hat{q}^{-1} \otimes G_q \otimes \hat{q} \quad (13)$$

where

$G_q = [0 \ 0 \ 0 \ 9.8]^T$: Quaternion representation of the gravity vector $G = [0 \ 0 \ 9.81]^T$.

Measurements of the estimated Earth's magnetic field \hat{h}_x , \hat{h}_y and \hat{h}_z can be calculated such as:

$$\hat{h} = [0 \ \hat{h}_x \ \hat{h}_y \ \hat{h}_z]^T = \hat{q}^{-1} \otimes m_q \otimes \hat{q} \quad (14)$$

where

$m_q = [0 \ m_x \ 0 \ m_z]^T$: Quaternion representation of the Earth's magnetic field $m = [m_x \ 0 \ m_z]^T$.

The minimization of the modeling error $\delta(\hat{q})$ is performed from a regression method that minimizes the scalar squared error criterion function $\xi(\hat{q})$ related to $\delta(\hat{q})$:

$$\xi(\hat{q}) = \delta(\hat{q})^T \delta(\hat{q}) \quad (15)$$

In this chapter, the Levenberg Marquardt Algorithm is used to minimize the non-linear function $\xi(\hat{q})$. This choice reflects the robustness demonstrated by this algorithm compared to other methods such as Gauss-Newton or gradient [30].

The unique solution to this problem can be written in the following form [31]:

$$\eta(\hat{q}) = K\delta(\hat{q}) \quad (16)$$

where $K = k [X^T X + \lambda I_{3 \times 3}]^{-1} X^T$ is the gain of the filter used to minimize the error $\delta(\hat{q})$.

$X \in \Re^{6 \times 3}$ is the Jacobian matrix defined by:

$$X = -2 \begin{bmatrix} [f^\times] & [h^\times] \end{bmatrix}^T = -2 \begin{bmatrix} 0 & -f_z & f_y & 0 & -h_z & h_y \\ f_z & 0 & -f_x & h_z & 0 & -h_x \\ -f_y & f_x & 0 & -h_y & h_x & 0 \end{bmatrix}^T \quad (17)$$

The constant λ is chosen to ensure the non-singularity of the minimization problem. The constant k determines the crossover frequency of the latter. It is used to tune the balance between measurement noises suppression and response time of the filter. Generally, it combines low bandwidth accelerometer/magnetometer readings with high bandwidth gyroscope measurements. Notice that, the complementary filter has a better convergence when k is chosen

somewhere between 0.1 and 1 [4]. $\eta(\hat{q})$ represents a part of the correction term T . To achieve the quaternion product in (11), the term T must be of dimension 4. So, T is constructed as follows:

$$T = \begin{bmatrix} 1 & 0 & 0 & 0 & 0 & 0 & 0 \\ 0 & & & & & & \\ 0 & & K & & & & \\ 0 & & & & & & \end{bmatrix} \begin{bmatrix} 1 \\ \delta(\hat{q}) \end{bmatrix} \quad (18)$$

The scalar part of quaternion error is chosen to 1 to force the error quaternion to represent small angles of rotation [32]. Finally, the complementary filter can be written as follows:

$$(F): \begin{bmatrix} \dot{\hat{q}}_0 \\ \dot{\hat{q}}_1 \\ \dot{\hat{q}}_2 \\ \dot{\hat{q}}_3 \end{bmatrix} = \frac{1}{2} \begin{bmatrix} -(\hat{q}_1\omega_x + \hat{q}_2\omega_y + \hat{q}_3\omega_z) \\ (\hat{q}_0\omega_x - \hat{q}_3\omega_y + \hat{q}_2\omega_z) \\ (\hat{q}_3\omega_x + \hat{q}_0\omega_y - \hat{q}_1\omega_z) \\ (\hat{q}_1\omega_y - \hat{q}_2\omega_x + \hat{q}_0\omega_z) \end{bmatrix} \otimes \begin{bmatrix} 1 & 0 & 0 & 0 & 0 & 0 & 0 \\ 0 & & & & & & \\ 0 & & K & & & & \\ 0 & & & & & & \end{bmatrix} \begin{bmatrix} 1 \\ \delta(\hat{q}) \end{bmatrix} \quad (19)$$

5. EXPERIMENTAL VALIDATION

5.1. EXPERIMENTAL TOOLS FOR ATTITUDE ESTIMATION: INERTIAL MEASUREMENT UNIT (MTI-G)

In order to evaluate the efficiency of the proposed complementary filter in real world applications, an experimental setup was developed resorting to an inertial and magnetic sensor assembly. The goal is to obtain an estimation of the quaternion that represents the orientation of a rigid body and to investigate its accuracy under various conditions. For the experiments, an Inertial Measurement Unit (IMU) was employed. The *MTi-G* from Xsens Motion Technologies [33] is used. This MEMS device is a miniature, lightweight, 3D calibrated digital output sensor (3D acceleration from accelerometer, 3D angular rate from gyroscope, and 3D magnetic field data from magnetometer), a GPS enhanced Attitude and Heading Reference System with built-in bias, sensitivity, and temperature compensation. The *MTi-G* outputs data at a rate of 100Hz and records them on a computer (see Fig. 3). In addition, this device is designed to track the body 3D attitude output in quaternion representation using an embedded Kalman filter algorithm. The calibration procedure to obtain the gain, offsets and non-orthogonality of the sensors was

performed by the manufacturer of the sensor module.

It is important to note that the *MTi-G* device serves as tool for the evaluation of the complementary filter efficiency and cannot be suitable for use in Bio-logging field due to its dependence on an energy source as well as its heavy weight. In the following set of experiment, the calibrated data from the *MTi-G* are used as input to the complementary filter.

5.2. EVALUATION TEST AND ANALYSIS IN FREE MOVEMENT OF ANIMAL

In this set of experiments, the accuracy of the complementary filter is evaluated during the free motion of a domestic animal (a dog). The *MTi-G* is attached to the back of the animal with its *xyz* axes aligned with those of the dog. The path followed by the animal was carried out in a football stadium as shown in Fig. 4. Inertial/magnetic measurements and attitude (in quaternion representation) are recorded using the *MTi-G* during the motion of the dog (see Fig. 5) and transmitted to a computer via USB port. It should be noted that, based upon measurements recorded by the accelerometer, we note that the animal motion consists of two acceleration profiles, one corresponding to the low frequencies of motion (during walk) and the other rather to the high frequencies (during trot and canter). The acceleration profile varies between $[-15, 15 \text{ m/s}^2]$ for f_x and f_y and $[-5, +25 \text{ m/s}^2]$ for f_z . The increase in the acceleration level between the natural gaits is due to the Dynamic Body Acceleration a of the dog that is more important during the trot and the canter.

The recorded inertial and magnetic measurements from the *MTi-G* are used to estimate the attitude using the proposed complementary filter. The calculated attitude from the *MTi-G* is considered as reference of the dog's motion. Fig. 6 plots the evolution of the difference between the calculated quaternion using the *MTi-G* and the one estimated by the proposed approach. Although some parts of the motion are with high dynamics, we can remark that the errors on quaternion's components don't exceed 0.03 on q_0 , q_1 , q_2 and 0.05 on q_3 . For more clarity to the reader, we also represent the attitude estimation results of the same movement using the Euler angles (roll, pitch and yaw). Fig. 7 shows the evolution of the difference between the Euler angles estimated by the complementary filter and the *MTi-G*.

It is clear that this mismatch between the estimated attitude by our approach and the *MTi-G* is small. Then, one can conclude about the performance of the complementary filter in attitude estimation of the animal body even in dynamic situations. Although our approach didn't exploit

a GPS data as done in *MTi-G*, it is able to reconstruct the orientation of the dog given by the *MTi-G* with a small error.

6. TOWARD THE 3D POSITION ESTIMATION IN PEDESTRIAN LOCOMOTION

In this chapter, we focus on the problem of 3D position estimation of a mobile with pedestrian locomotion (human walking) using a dead reckoning approach. Our motivation is to go toward the estimation of the animal's 3D position in Bio-logging. In this context, a position estimation approach is proposed based only on proprioceptive measurements provided by a 3-axis accelerometer, a 3-axis magnetometer and a 3-axis gyroscope, where the Dynamic Body Acceleration is integrated to estimate at first the linear velocity and then the position. The complementary filter approach, presented in the previous section, is used to estimate the body attitude that is necessary to reconstruct the Dynamic Body Acceleration. The obtained results are satisfactory and remain promising for terrestrial animal in Bio-logging application.

6.1. 3D POSITION ESTIMATION APPROACH USING A DEAD RECKONING TECHNIQUE

The proposed approach is based on the dead reckoning technique [34]. It consists in deducing the position of a mobile from its last known position. Therefore, we used the physical relationship existing between the estimated Dynamic Body Acceleration of the mobile \hat{a} and its estimated position \hat{p} . It can be written using the following two equations:

$$\hat{v}(t) = \int_{T_1}^{T_2} \hat{a}(t).dt \quad (20)$$

$$\hat{p}(t) = \int_{T_1}^{T_2} \hat{v}(t).dt \quad (21)$$

where \hat{v} represents the estimated linear velocity of the mobile and $[T_1 ; T_2]$ denotes the sampling period.

The Dynamic Body Acceleration of the mobile \hat{a} can be deduced from the equation (4):

$$\hat{a} = \text{inv}\left(M_N^B(\hat{q})\right)f - G \quad (22)$$

where $M_N^B(\hat{q})$ is the rotation matrix defined in (3). It is expressed in terms of the estimated

quaternion from the complementary filter. $G \in \mathfrak{R}^3$ is the gravity vector and $f \in \mathfrak{R}^3$ is the accelerometer measurements.

Based solely on equations (20) and (21), a significant and fast drift appears at the position estimation. This drift was predictable; it is mainly due to measurement noise in the accelerometer signal f and their numerical integration in (20) and (21). To overcome this problem, one introduces a correction step usually proposed for pedestrian navigation [35], [36] in the case of human and terrestrial animal locomotions (see Fig. 8). The idea is to use an Inertial Measurement Unit attached to the human's foot. The accelerometer measurements f allow us to detect the moments when the acceleration norm $\|f\|_2$ equals gravity. At these moments, theoretically the Dynamic Body Acceleration \hat{a} and the linear velocity \hat{v} vanish since the foot reaches the ground (see Fig. 9). But in reality, they stay slightly different from zero at these moments. Therefore, a correction step is applied to reset the linear velocity to zero at these moments.

First, we calculate the squared norm of the measured acceleration $\|f\|_2^2$ by using the following formula:

$$\chi = \|f\|_2^2 = f_x^2 + f_y^2 + f_z^2 \quad (23)$$

one then calculate the means mo of χ over a range of samples e :

$$mo = \frac{\chi}{e} \quad (24)$$

Then, the variance of this squared norm is computed on a sliding window by using the following equation [37]:

$$V_e(j) = \frac{1}{e-1} \sum_{i=j-e+1}^{i=j} (\chi_i - mo_j)^2 \quad (25)$$

where χ_i is the squared norm of the measured acceleration f and mo_j is the means of χ_i over a chosen range of samples e . The variance of the squared norm is used to detect significant moments of movement of the subject such as where the foot touches the ground (Dynamic Body Acceleration theoretically equal to zero). The samples interval e must be carefully chosen so

that the test of the variance is sufficiently sensitive to slow and rapid changes of the accelerometer signal.

To detect the moments when the estimated Dynamic Body Acceleration \hat{a} vanishes, the following condition is imposed:

$$V_e < L \quad (26)$$

When condition (26) is performed, it is necessary to reset the components of velocity vector \hat{v} to zero before using the equations (20) and (21). Otherwise, the integration procedure using these two equations is normally done without resetting the velocity.

6.2. EXPERIMENTAL RESULTS IN THE CASE OF HUMAN PEDESTRIAN LOCOMOTION

To examine the accuracy of the position estimation by the proposed approach above, we perform experimental trials in the case of human walking. The Inertial Measurement Unit *MTi* [33] was used to collect magnetic and inertial measurements that are used firstly to estimate the attitude by the complementary filter. This device has the same characteristics as the *Mti-G*. The *MTi* is attached to the end of the human's foot as shown in Fig. 10 and used after to record data during an episode of walking during a few minutes. In this case, it is possible to obtain the norm of the Dynamic Body Acceleration \hat{a} near to zero each time the foot touches the ground. To get an accurate reference of 3D walking trajectory, we chose to perform a known one along the corridors of our laboratory CReSTIC in Reims as shown in Figure 11. This trajectory takes the form of a rectangle with a size $\approx 2 \times (22 \text{ meters} \times 19 \text{ meters})$.

To estimate the attitude of the human's foot during the 3D walking trajectory, we used the complementary filter approach proposed in the previous section. The estimated attitude \hat{q} is then used to calculate the Dynamic Body Acceleration from (22). Then we calculated the values of the squared norm of the measured acceleration χ_i by using (23). The means mo_j for this acceleration is then calculated through (24) with the range of samples $e = 8$. Finally, the values of variance V_e are derived using (25).

Fig. 12 includes the squared norm of the measured acceleration χ_i , the means mo_j , the variance $V_e(j)$ and the moments where the foot touches the ground. Finally, we have applied equations (20) and (21) to extract the estimated position of the person along his trajectory. At each

integration step, the condition (26) is verified and when it is checked the velocity vector \hat{v} is initialized to zero. The limit L in this condition is experimentally set (depending on the nature of human walking) in order to adequately detect and differentiate the phases of walking and rest (the foot touches the ground). Figure 12 shows the validity of the proposed approach to locate the phase where the foot reaches the ground. Indeed, the detector shown in this figure is set to 1 when the foot touches the ground and changes to 0 during walk. The linear velocity estimation with and without the correction step is plotted in Fig. 13. The improvement provided by this step is obvious in all three axes (solid line versus dashed line). If this reset is not done, the observed differences are due to the integration of noise in the accelerometer measurements. We calculated in a first step the 3D position of the person using the usual integration procedure from equations (20) and (21) without correction step. Note that we have chosen to begin the estimation of position from the initial point $(0,0,0)$. We show in Fig. 14 the estimated 3D trajectory. A rapid and total divergence in estimation of position is observed in this figure. The error is about 300 meters on the X, Y and Z-axis. Fig. 15 illustrates the improvement in the estimation of 3D position after adding the correction step of the velocity using the condition (26). This procedure allows obtaining an estimation of position with an absolute error ranging between 5 and 10 meters on the X and Y-axes and 30 cm on the Z-axis.

7. CONCLUSION

This paper focused principally to the 3D motions estimation of rigid body. The application in mind concerns Bio-logging and aims to track posture and orientation of free-ranging animals during their natural lives.

Firstly, a quaternion-based complementary filter for the rigid body attitude estimation has been designed. The proposed state estimation algorithm adds to the data from a 3-axis accelerometer and a 3-axis magnetometer the one provided by a 3-axis gyroscope. The main idea is to combine a strap-down system, based on the time integral of angular velocity, with the Levenberg Marquardt Algorithm. The efficiency of the proposed approach is highlighted with a set of experiments on a domestic animal through sensor measurements provided by an Inertial Measurement Unit (MTi-G).

Secondly, the problem of 3D position estimation in the case of human pedestrian locomotion was addressed. The Dynamic Body Acceleration is integrated to estimate at first the linear velocity

and then the position. The complementary filter approach, presented in the previous section, is used to estimate the body attitude that is necessary to reconstruct the Dynamic Body Acceleration. The obtained results are satisfactory and remain promising for terrestrial animal in Bio-logging application.

ACKNOWLEDGEMENT

The authors would like to thank both the Alsace and Champagne-Ardenne regions within the framework of the project (NaviMeles) for their financial support.

REFERENCES

- [1] H. Zhou, H. Hu, N. D. Harris, and J. Hammerton, "Applications of wearable inertial sensors in estimation of upper limb movements," *Biomedical Signal Processing and control*, vol. 1, no. 1, pp. 22-32, 2006.
- [2] K. J. O'Donovan, R. Kamnik, D. T. O'Keeffe, and G. M. Lyons, "A inertial and magnetic sensor based technique for joint angle measurement," *Journal of Biomechanics*, vol. 40, no. 12, pp. 2604-2611, 2007.
- [3] W. T. Ang, P. K. Khosla, and C. N. Riviere, "Kalman filtering for real-time orientation tracking of handheld microsurgical instrument," *IEEE/RSJ International Conference on Intelligent Robots and Systems*, Sendai, Japan, 2004, pp. 2574-2580.
- [4] R. Mahony, T. Hamel, and J. M. Pflimlin, "Nonlinear complementary filters on the special orthogonal group," *IEEE Transactions on Automatic Control*, vol. 53, no. 5, pp. 1203-1218, 2008.
- [5] C. Rutz, and G. C. Hays, "New frontiers in biologging science," *Biology letters*, vol. 5, no. 3, pp. 289-291, 2009.
- [6] Y. Ropert-Coudert, M. Beaulieu, N. Hanuise, and A. Kato, "Diving into the world of biologging," *Endangered Species Research*, vol. 10, pp. 21-27, 2009.
- [7] L. G. Halsey, Y. Handrich, A. Fahlman, A. Schmidt, C. A. Bost, R. L. Holder, A. J. Woakes, and P. J. Butler, "Fine-scale analyses of diving energetics in king penguins *Aptenodytes patagonicus*: how behaviour affect costs of a foraging dive," *Marine Ecology Progress Series*, vol. 344, pp. 299-309, 2007.

- [8] C. A. Bost, Y. Handrich, P. J. Butler, A. Fahlman, L. G. Halsey, A. J. Woakes, and Y. Ropert-Coudert, "Change in dive profiles as an indicator of feeding success in king and Adélie penguins," *Deep-Sea Research II*, vol. 54, no. 3-4, pp. 248-255, 2007.
- [9] B. J. Le Boeuf, D. E. Crocker, D. P. Costa, S. P. Blackwell, P. M. Webb, and D. S. Houser, "Foraging ecology of northern elephant seals," *Ecological Monographs*, vol. 70, no. 3, pp. 353-382, 2000.
- [10] G. L. Kooyman, "Genesis and evolution of bio-logging devices: 1963-2002," *Memoirs of the National Institute of Polar Research*, vol. 58, pp. 148-154, 2004.
- [11] G. H. Elkaim, E. B. Decker, G. Oliver, and B. Wright, "Marine Mammal Marker (MAMMARK) dead reckoning sensor for In-Situ environmental monitoring," *Proceedings of IEEE Position, Location and Navigation Symposium*, Monterey, April 2006, pp. 976-987.
- [12] M. P. Johnson, and P. L. Tyack, "A digital acoustic recording tag for measuring the response of wild marine mammals to sound," *IEEE Journal of Oceanic Engineering*, vol. 28, no. 1, pp. 3-12, 2003.
- [13] S. Watanabe, M. Isawa, A. Kato, Y. Coudert, and Y. Naito, "A new technique for monitoring the behaviour of terrestrial animals; a case study with the domestic cat," *Applied Animal Behaviour Science*, vol. 94, pp. 117-131, 2005.
- [14] R. Wilson, E. L. C. Shepard, and N. Liebsch, "Prying into the intimate details of animal lives: use of a daily diary on animals," *Endangered Species Research*, vol. 4, pp. 123-137, 2008.
- [15] H. Fourati, N. Manamanni, L. Afilal, and Y. Handrich, "A rigid body attitude estimation for Bio-logging application: A quaternion-based nonlinear filter approach," *IEEE/RSJ International conference on Intelligent Robots and Systems IROS'09*, St. Louis, USA, October 2009, pp. 558-563.
- [16] H. Fourati, N. Manamanni, L. Afilal, and Y. Handrich, "A nonlinear filtering approach for the attitude and Dynamic Body Acceleration estimation based on inertial and magnetic sensors: Bio-logging application," *IEEE Sensors Journal*, vol. 11, no.1, pp. 233-244, 2011.
- [17] Y. Naito, "New steps in bio-logging science," *Memoirs of National Institute of Polar Research, special issue*, vol. 58, pp. 50-57, 2004.
- [18] H. Goldstein, *Classical Mechanics*. 2nd Ed. Reading, MA: Addison-Wesley, 1980.

- [19] M. S. Grewal, L. R. Weill, and A. P. Andrews, *Global positioning systems, inertial navigation, and integration*. John Wiley & Sons, Inc., 2001.
- [20] J. B. Kuipers, *Quaternion and Rotation Sequences*. Princeton, NJ: Princeton University Press, 1999.
- [21] S. Beeby, G. Ensell, M. Kraft, and N. White, *MEMS Mechanical Sensors*. Artech House House Publishers, 2004.
- [22] J. F. Guerrero-Castellanos, "Estimation de l'attitude et commande borne en attitude d'un corps rigide: Application à un hélicoptère à quatre rotors, " Ph.D dissertation, Joshep Fourier University, Grenoble, France, 2008.
- [23] Astrosurf, September 2009. Available: <http://www.astrosurf.com>
- [24] D. H. Titterton, and J. L. Weston, *Strapdown Inertial Navigation Technology*. 2nd Ed, UK: The institution of Electrical Engineers, 2004.
- [25] H. Fourati, N. Manamanni, L. Afilal, and Y. Handrich, "Posture and body acceleration tracking by inertial and magnetic sensing: Application in behavioural analysis of free-ranging animals," *Biomedical Signal Processing and Control (BSPC)*, vol. 6, no. 1, pp. 94-104, 2011.
- [26] R. G. Brown, and P. Y. C. Hwang, *Introduction to Random Signal and Applied Kalman Filtering*. 3rd Ed. New York: John Wiley, 1997.
- [27] M. D. Shuster, "A survey of attitude representations," *Journal of the Astronautical Science*, vol. 41, no. 4, pp. 493-517, 1993.
- [28] H. Fourati, N. Manamanni, A. Benjemaa, L. Afilal, and Y. Handrich, "A quaternion-based Complementary Sliding Mode Observer for attitude estimation: application in free-ranging animal motions," *49th IEEE Conference on Decision and Control (CDC)*, Atlanta, USA, pp. 5056-5061, 2010.
- [29] H. Fourati, N. Manamanni, L. Afilal, P. Van Hove, and Y. Handrich, "A complementary observer-based approach for the estimation of motion in rigid bodies using inertial and magnetic sensors," *IEEE Multi-Conference on Systems and Control (Conference on Control Applications) (IEEE MSC-CCA)*, Yokohama, Japan, pp. 422-427, 2010.
- [30] J. E. Dennis, Jr. and Robert B. Schnabel. *Numerical Methods for Unconstrained Optimization and Nonlinear Equations*, Prentice Hall, Englewood, NJ, 1983.
- [31] D. W. Marquardt, "An Algorithm for the Least-Squares Estimation of Nonlinear Parameters," *SIAM Journal of Applied Mathematics*, vol. 11, no. 2, pp. 431-441, 1963.

- [32] J. Deutschmann, I. Bar-Itzhack, and K. Galal, "Quaternion normalization in spacecraft attitude determination," *AIAA Astrodynamics Conference*, Washington, USA, 1992, pp. 27-37.
- [33] Xsens Technologies, June 2011. Available: <http://www.xsens.com>
- [34] U. Steinhoff, and B. Schiele, "Dead reckoning from the pocket - An experimental study," *IEEE International Conference on Pervasive Computing and Communications (PerCom)*, Mannheim, Germany, pp. 162-170, 2010.
- [35] Q. Ladetto, "Capteurs et Algorithmes pour la localisation Autonome en Mode Pédestre," Ph.D dissertation, Ecole Polytechnique Fédérale de Lausanne (EPFL), 2003.
- [36] L. Ojeda, and J. Borenstein, "Non-GPS Navigation for Security Personnel and First Responders," *Journal of Navigation*, vol. 60, no. 3, pp. 391-407, 2007.
- [37] S. Rajagopal, "Personal Dead Reckoning System with Shoe Mounted Inertial Sensors," Master's Degree Project, Stockholm, Sweden, 2008.

FIGURE CAPTIONS

Fig.1 Schematic diagram of how an Inertial Measurement Unit is attached to a penguin

Fig. 2 The coordinate system (B) of a rigid body represented in the Earth- fixed frame (N)

Fig. 3 Inertial Measurement Unit *MTi-G*

Fig. 4 The *MTi-G* attached to the back of the dog - Description of the dog motion

Fig. 5 Inertial and magnetic measurements recorded from the *MTi-G*

Fig. 6 Differences between quaternion's components estimates produced by the complementary filter and the *MTi-G* during the motion of the dog

Fig. 7 Differences between Euler angles estimates produced by the complementary filter and the *MTi-G* during the motion of the dog

Fig. 8 Terrestrial animal with the Inertial Measurement Unit attached to the paw

Fig. 9 Key phases in a stride. During ΔT , all velocity components of point A in the sole of the boot are zero

Fig. 10 Inertial Measurement Unit *MTi* attached to the foot of a subject during displacement

Fig. 11 3D trajectory of walking

Fig. 12 The squared norm of the measured acceleration χ_i , the average mo_j , the variance $V_e(j)$ and the moments of step detection (detector d)

Fig. 13 Estimation of the linear velocity \hat{v} with and without correction step

Fig. 14 Experimental result of 3D walking trajectory estimation without correction step

Fig. 15 Experimental result of 3D walking trajectory estimation with correction step

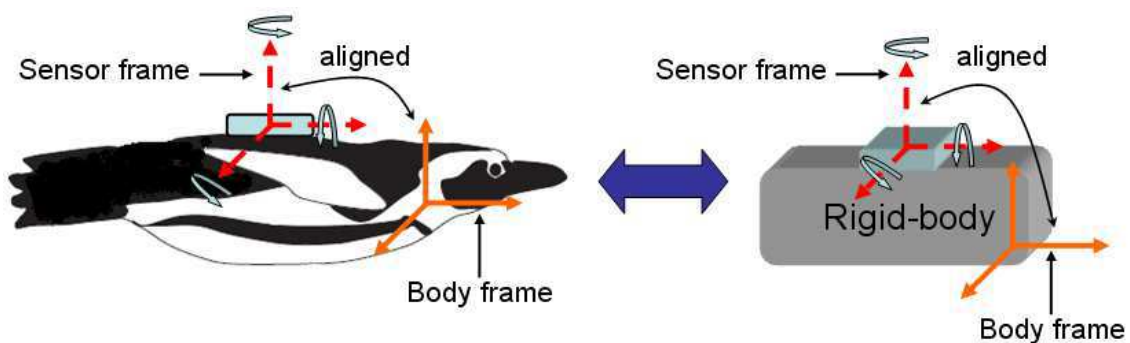


Fig.1 Schematic diagram of how an Inertial Measurement Unit is attached to a penguin

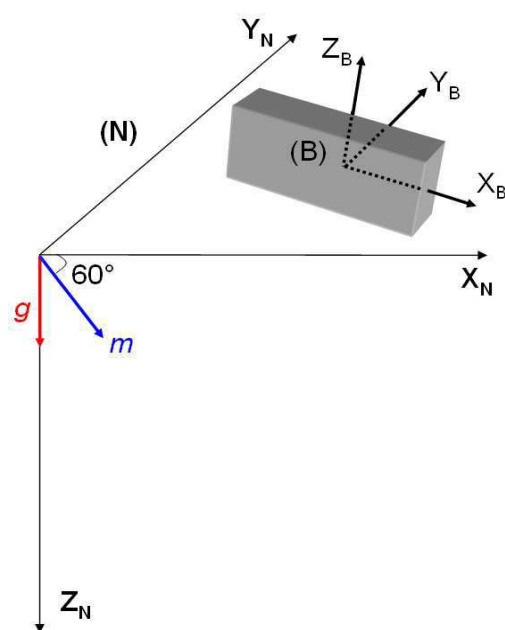


Fig. 2 The coordinate system (B) of a rigid body represented in the Earth- fixed frame (N)

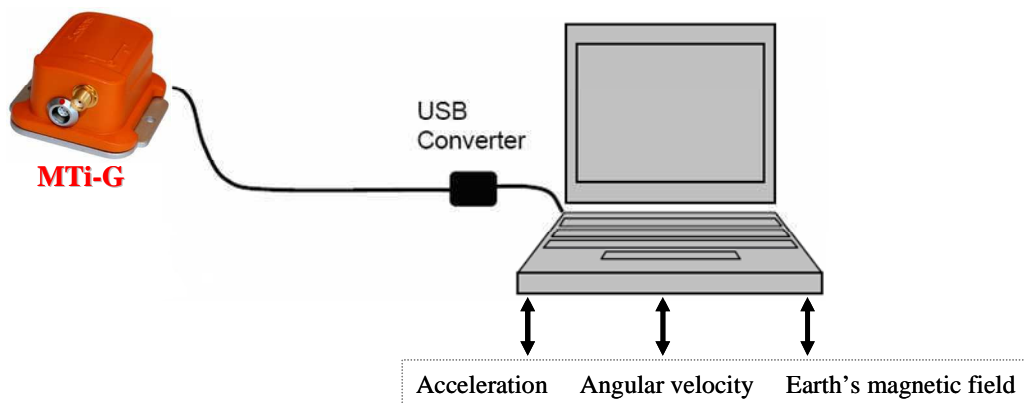


Fig. 3 Inertial Measurement Unit *MTi-G*

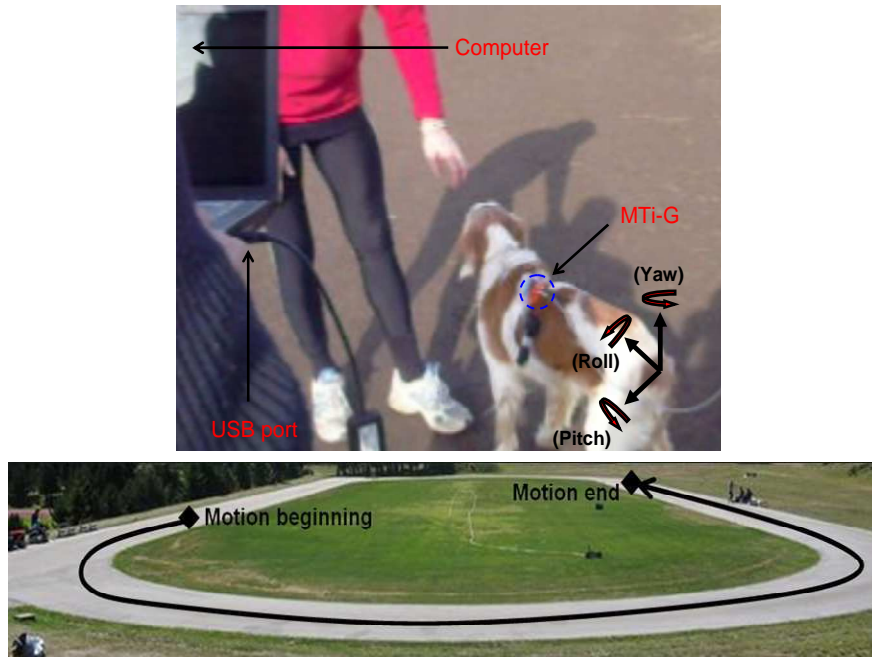


Fig. 4 The *MTi-G* attached to the back of the dog - Description of the dog motion

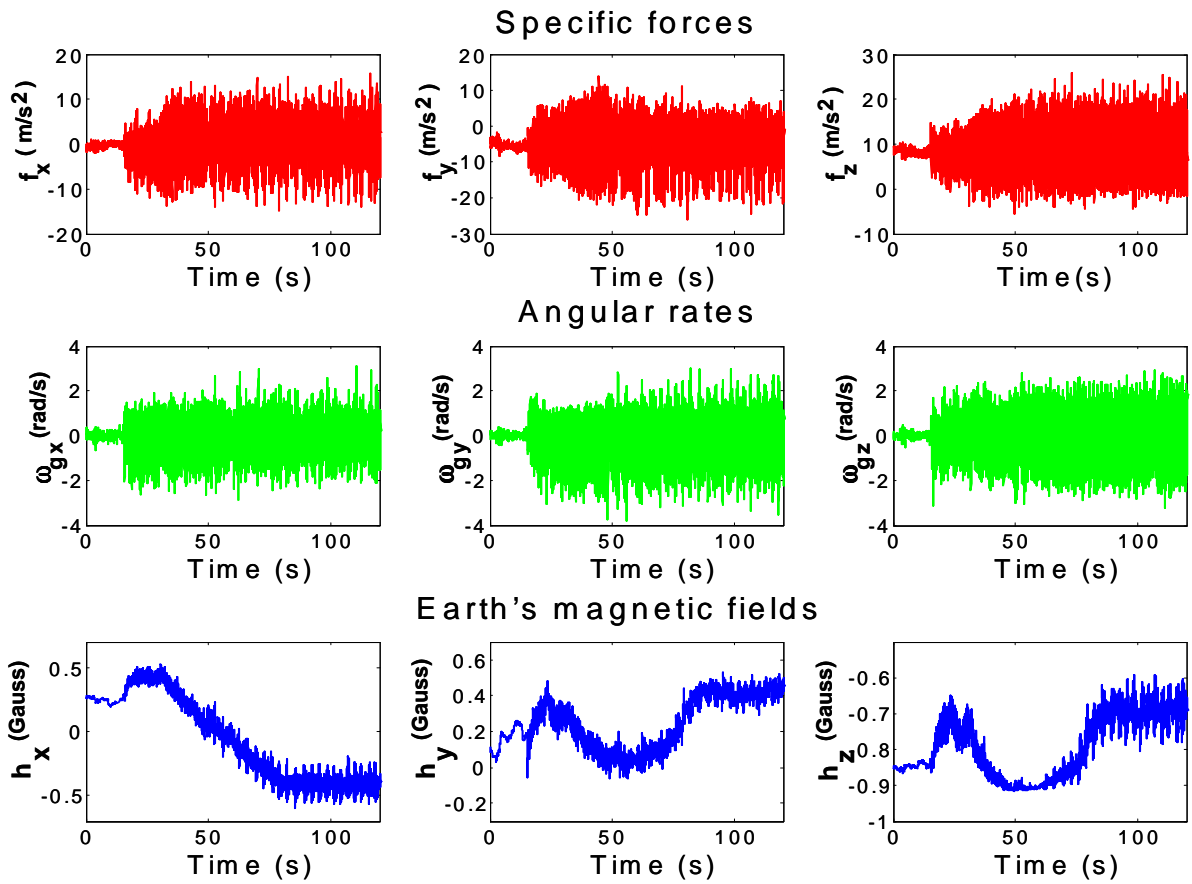


Fig. 5 Inertial and magnetic measurements recorded from the *MTi-G*

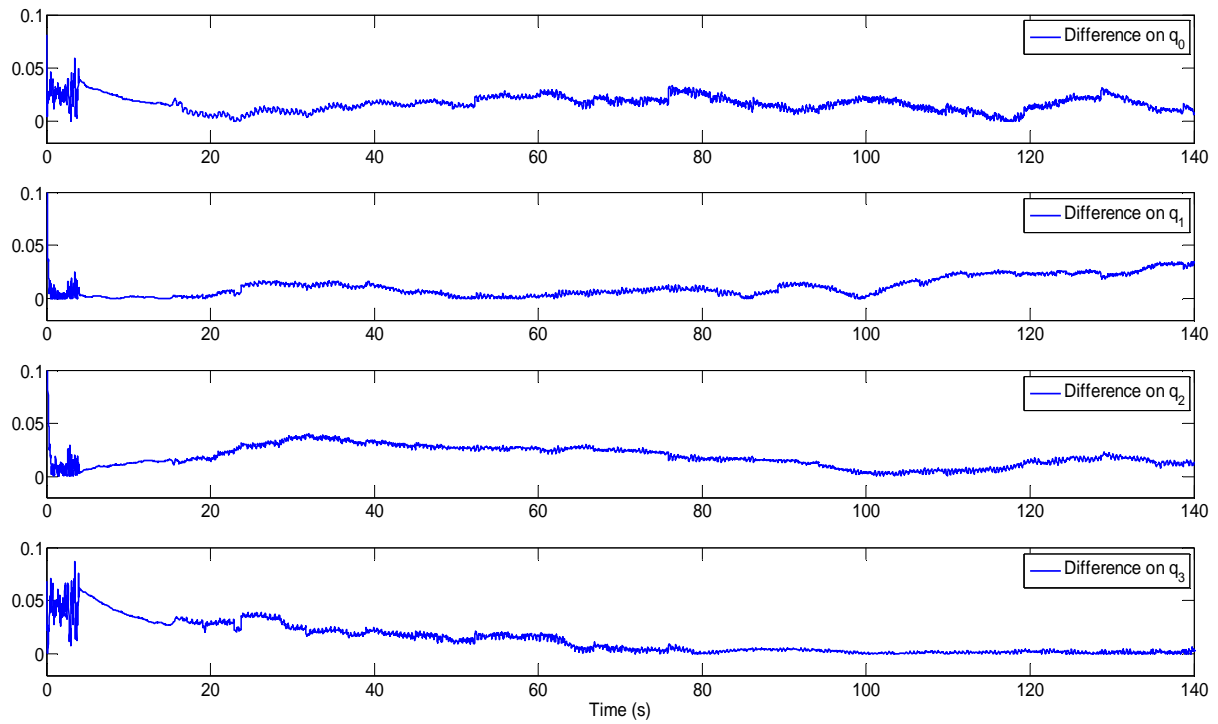


Fig. 6 Differences between quaternion's components estimates produced by the complementary filter and the *MTi-G* during the motion of the dog

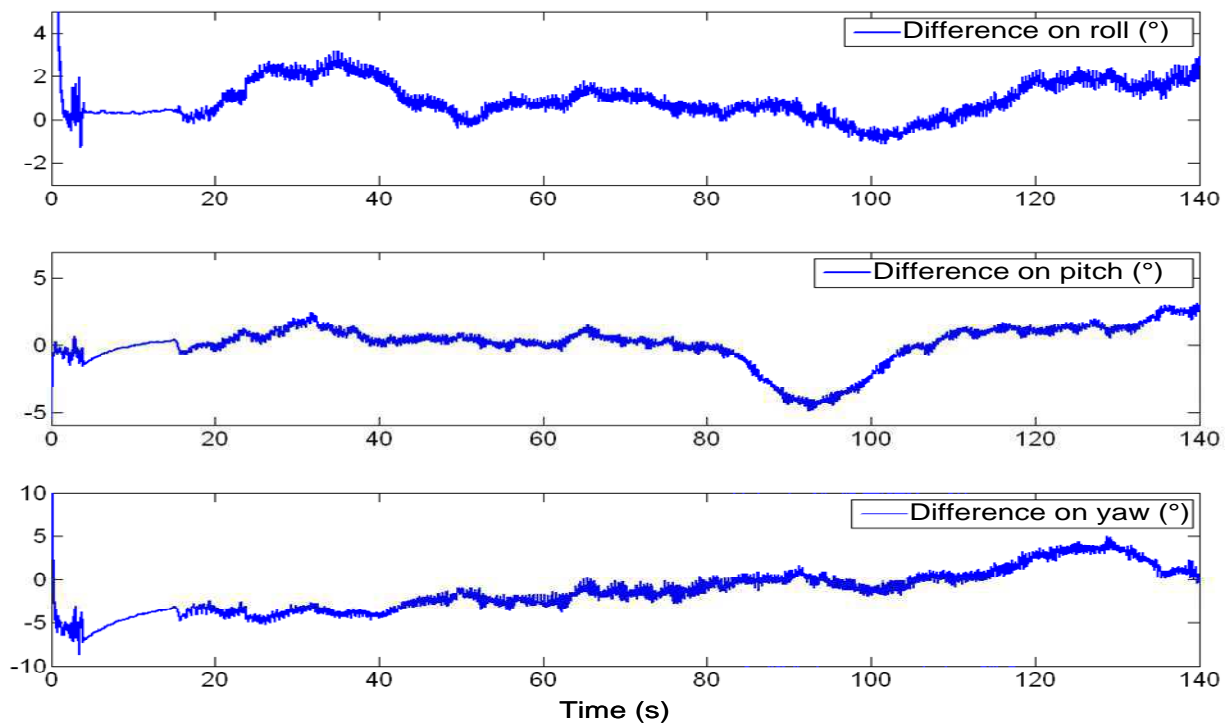


Fig. 7 Differences between Euler angles estimates produced by the complementary filter and the *MTi-G* during the motion of the dog

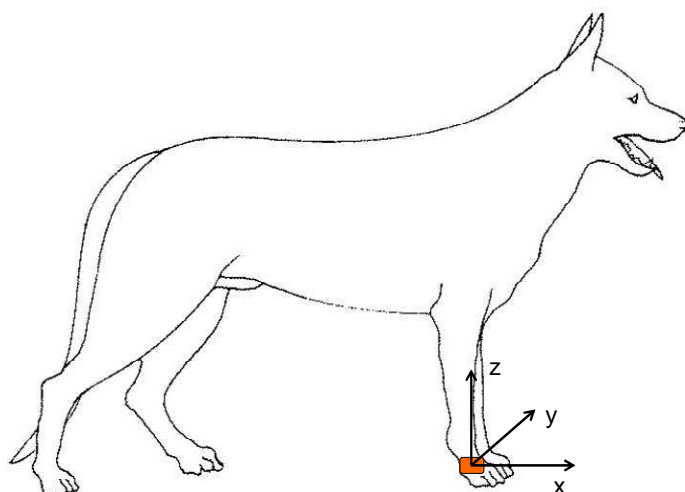


Fig. 8 Terrestrial animal with the Inertial Measurement Unit attached to the paw

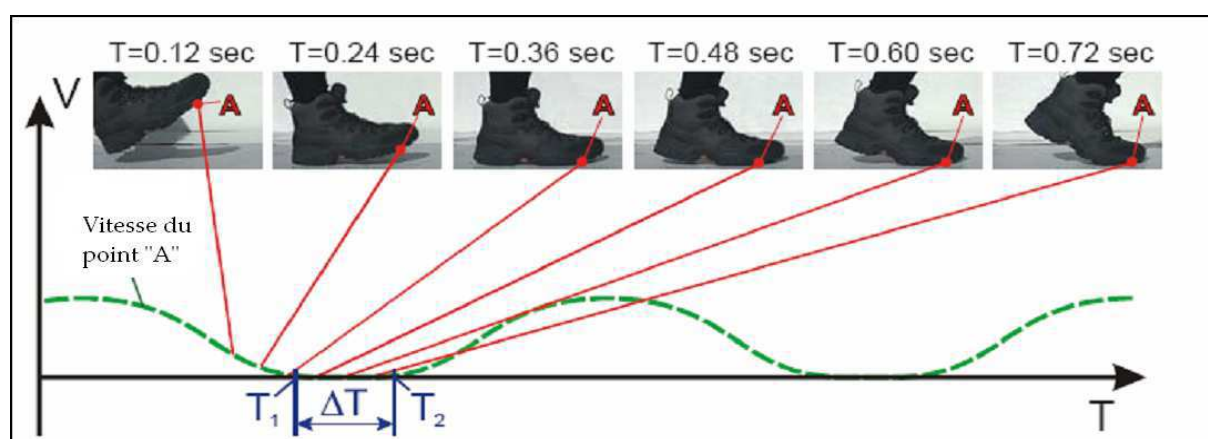


Fig. 9 Key phases in a stride. During ΔT , all velocity components of point A in the sole of the boot are zero



Fig. 10 Inertial Measurement Unit *MTi* attached to the foot of a subject during displacement

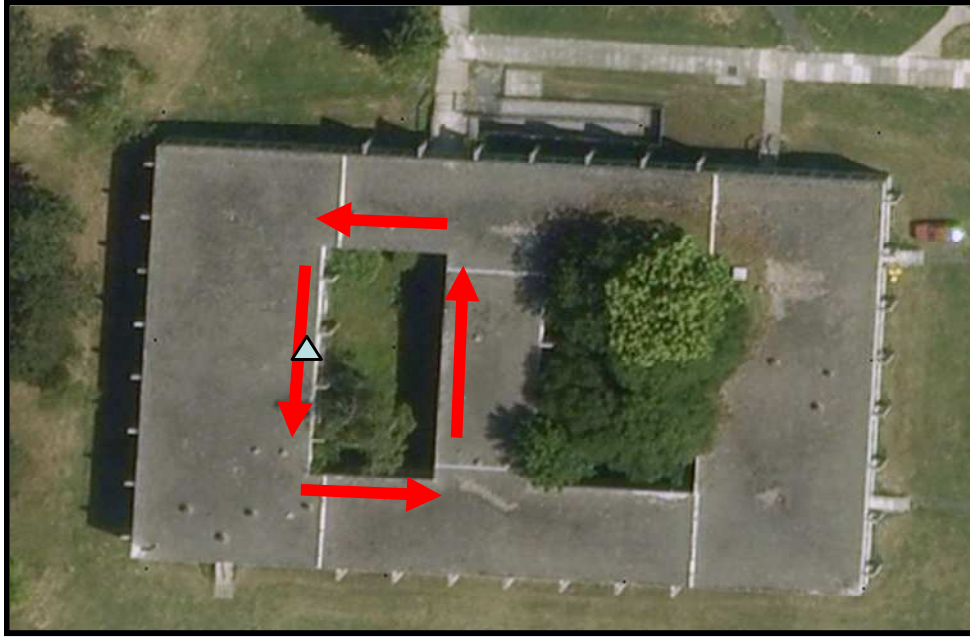


Fig. 11 3D trajectory of walking

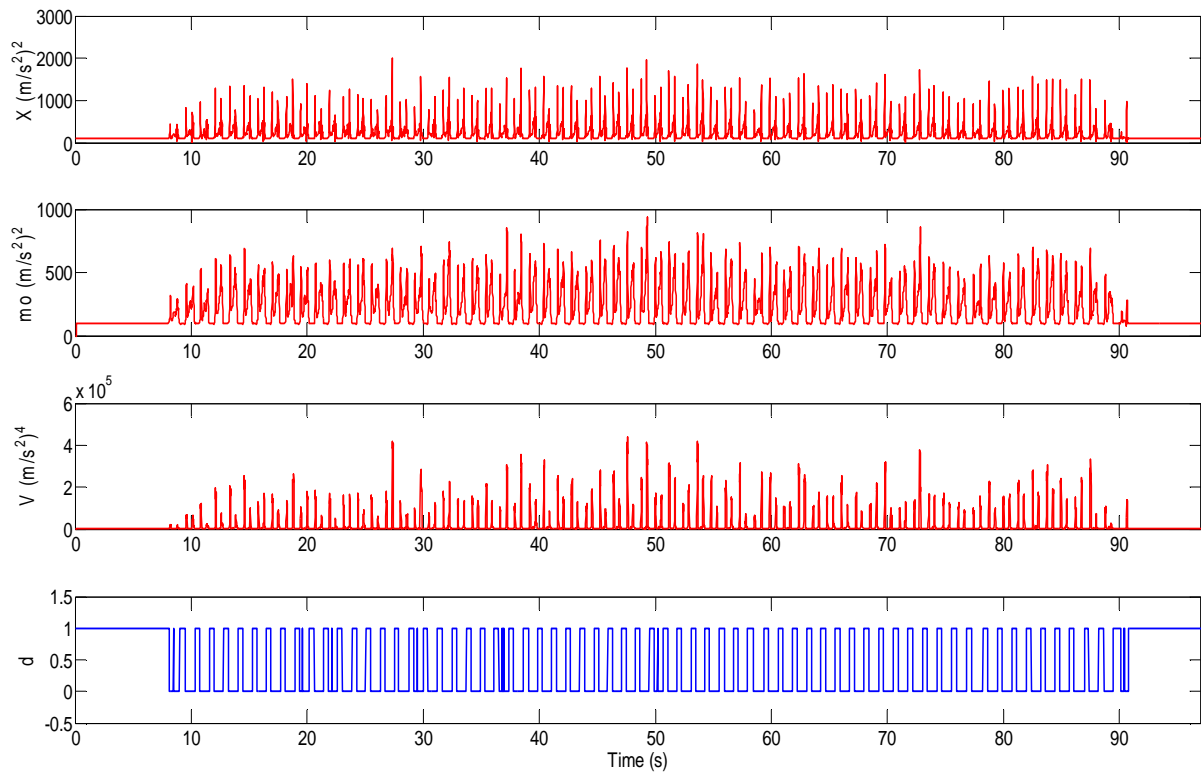


Fig. 12 The squared norm of the measured acceleration χ_i , the average mo_j , the variance $V_e(j)$ and the moments of step detection (detector d)

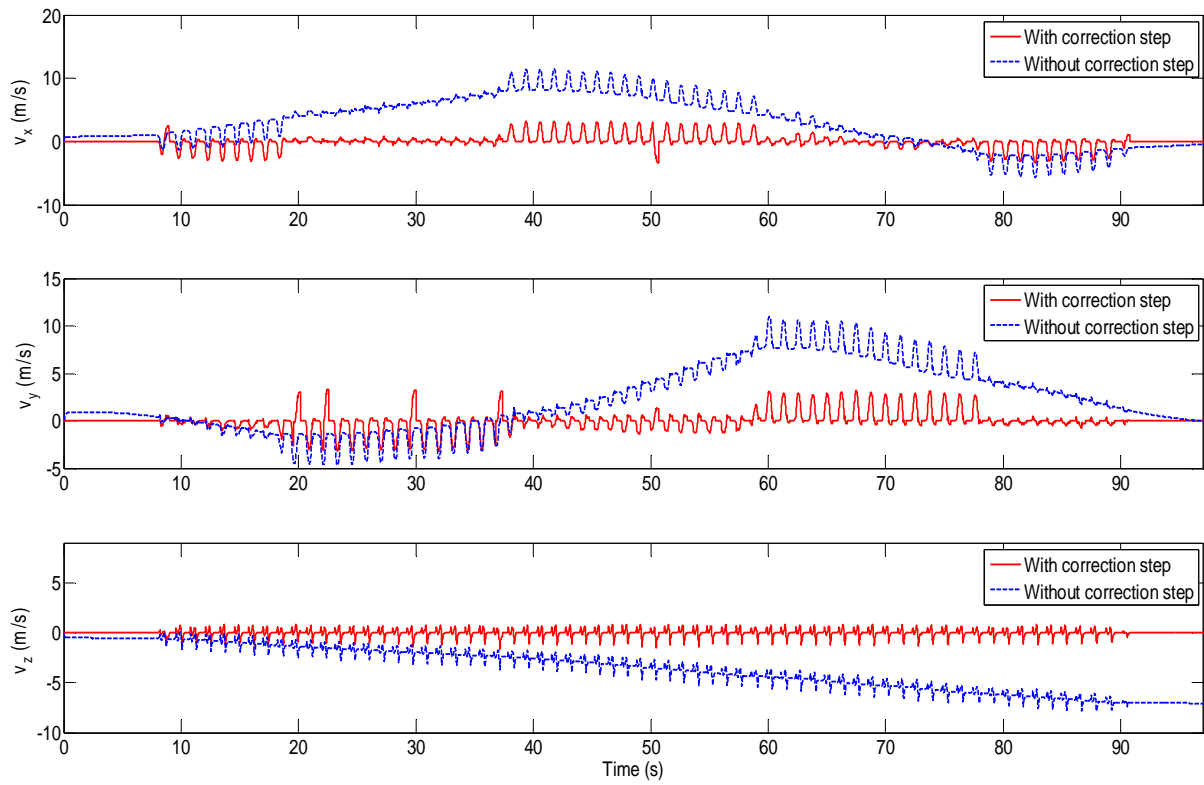


Fig. 13 Estimation of the linear velocity \hat{v} with and without correction step

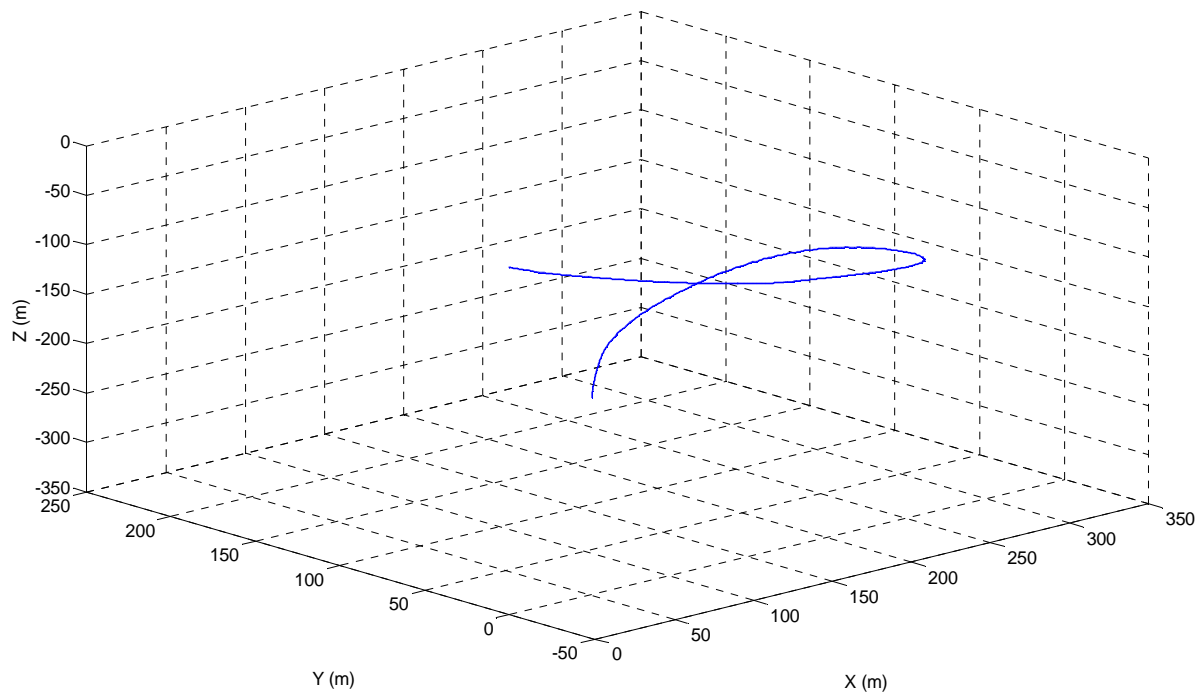


Fig. 14 Experimental result of 3D walking trajectory estimation without correction step

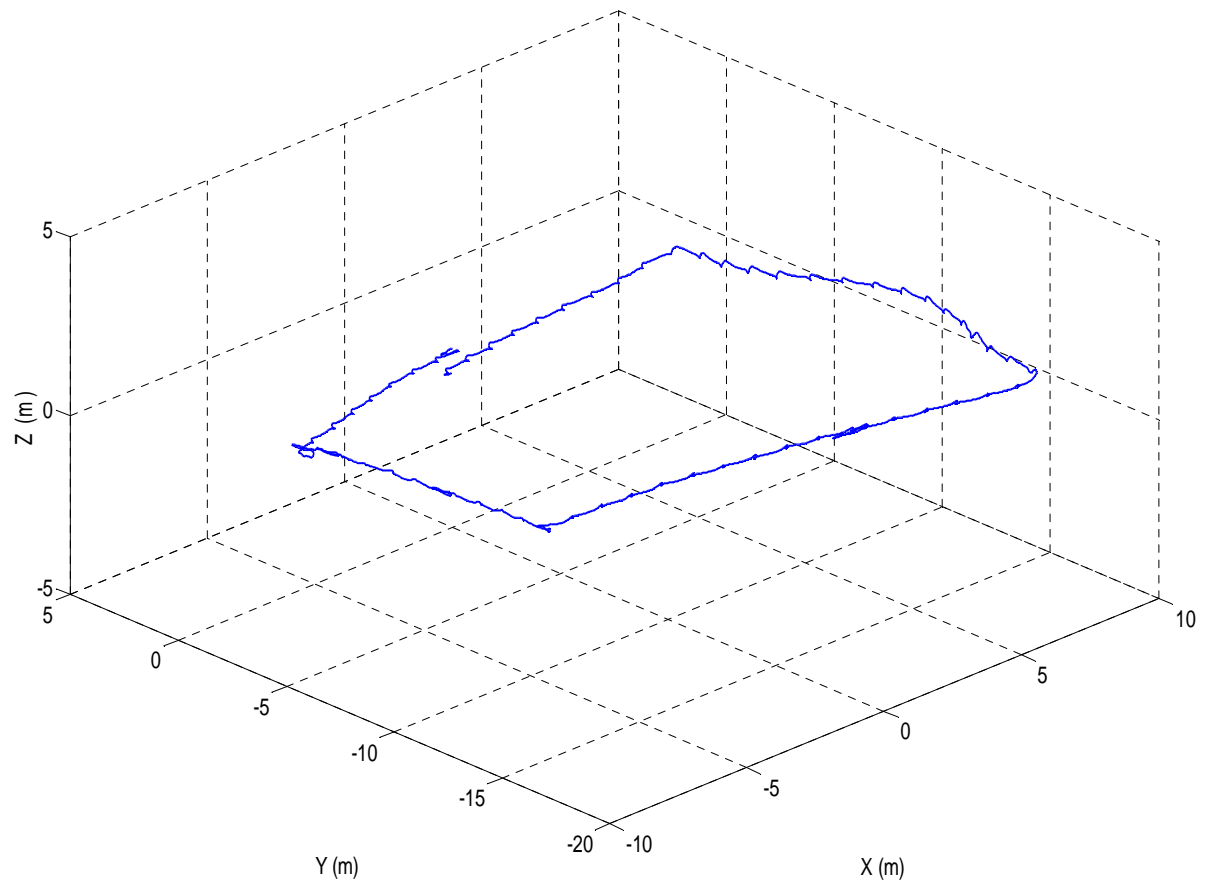


Fig. 15 Experimental result of 3D walking trajectory estimation with correction step